Progress In Electromagnetics Research C, Vol. 67, 143–152, 2016

A Novel Wideband Bandpass Filter Using Coupled Lines and T-Shaped Transmission Lines with Wide Stopband on Low-Cost Substrate

Lahcen Yechou[1, *], Abdelwahed Tribak[1], Mohamed Kacim[1], Jamal Zbitou[2], and Angel Mediavilla Sanchez[3]

Abstract—This paper presents the design, simulation, fabrication and measurement of a wideband bandpass filter with wide stopband performance operating at 3.5 GHz. The proposed filter consists of two parallel coupled lines (T-PCL) centred by T-inverted shape. The location of transmission zeros can be adjusted by varying the physical lengths of T-inverted shape to improve the filter selectivity. The wide bandwidth is achieved through enhanced coupling between the input and the parallel coupled lines. Due to the transmission zeros in the lower and upper stopbands, the filter exhibits good performance including an extremely wide stopband and sharp attenuations near the passband together with low insertion and good return losses in the passband. The filter performance is investigated numerically by using CST-MWS. Finally, the microstrip wideband BPF with minimum insertion losses 0.3 dB, centred at 3.5 GHz with a 3-dB fraction bandwidth of 70% and four transmission zeros is implemented and verified experimentally. In addition, good agreement between the simulated and measured results is achieved.

1. INTRODUCTION

In modern wireless communication systems, high-performance bandpass filters with compact size, wide bandwidth, low loss, and high selectivity are very popular for most of the radio frequency RF and microwave engineers [1]. Microstrip wideband bandpass filters (WB-BPFs) are important and key components for the wideband wireless communication systems. With the progressive development of modern wireless communications, the radio frequency RF spectrum has become increasingly crowded. Wireless transceivers are required to operate in a non single number of bands in order to allow users to adapt a terminal for achieving different services, and consequently the need for RF wideband filters has also increased. In planar technology, compact wideband filters can be implemented using different basic approaches [2]. However, RF filters present several problems of spurious responses mainly due to the presence of the second harmonic if such conventional designs are used. Various filters are designed with different methods, in order to obtain wide bandwidth, wide upper stopband, and high selectivity [3–21]. Methods using the three-line microstrip coupled structure, split ring resonators (SRRs), multimode resonators, open-ended stubs, transversal signal interaction concepts and defected ground surface have been introduced for the WBPF designs with good wideband responses. However, designs of WBPF with high selectivity and wide stopband remain as challenges.

A class of wideband BPFs with wide stopband is proposed based on a novel stepped coupled line structure in [4, 8, 18]; a modified quarter-wavelength stepped-impedance resonator is proposed in [4].

Received 22 June 2016, Accepted 3 September 2016, Scheduled 22 September 2016

* Corresponding author: Lahcen Yechou (lahcen.yechou@gmail.com).

[1] STRSS Lab., INPT-Institut National of Post and Telecommunications, Rabat, Morocco. [2] LMEET Laboratory, FPK/FST of Settat Hassan 1ST University, Morocco. [3] DICOM Laboratory, University of Cantabria Santander, Spain.

Multiple transmission zeros and the suppression of harmonics can be obtained in the stopband for enhancing frequency selectivity. This filter has only an FWB of 25%. In [18], a wideband equal-ripple filter used cascaded serial and shunt transmission line sections to produce wide fractional bandwidth (FBW) of 54% and transmission zeros near the passband edge. This filter has several drawbacks of large size and complexity in configuration. In [9], a quad-mode wideband BPF with about 43.3% fractional bandwidth based on a stub-loaded MMR is constructed using two parallel coupled feeding lines connected with a Tshaped resonator. In [13], the designed filter having an FWB of 36.1% was composed of a modified dual-mode patch resonator and a pair of input/output DMSs with dual-bandgap characteristics. Novel defected ground structures were used to design a wideband BPF with high selectivity in [16, 17, 20, 21]. In planar technology, compact wideband filters can be implemented using different basic approaches; however, these filters present several problems of spurious responses mainly due to the presence of the second harmonic if such conventional designs are used. But the filters mentioned above have a narrow bandwidth, relative narrow stopband, relatively large in size, and cannot suppress the high order harmonics.

In this paper, a WBPF with excellent selectivity based on two parallel coupled lines resonators centred by a T-inverted shape is proposed. An accurate equivalent circuit model of the proposed filter is investigated and demonstrates consistent results with full-wave simulation. Good wideband response with four transmission zeros can be achieved by the proposed T-inverted resonator. This coupled scheme can provide three transmission zeros in the upper stopband to better enhance the passband selectivity and stopband rejection level. Then, a WBPF is implemented on an FR4 substrate. Good agreement between the simulation and experiment results is achieved. In the following sections, we will present the different steps to design and t simulate the proposed wideband bandpass filter, and at the end a comparison between simulation and measurement results.

2. FILTER DESIGN AND ANALYSIS

Figure 1 shows the configuration of the proposed wideband bandpass filter with wide stopband. The basic element of this filter is a parallel coupled microstrip line, and the advantages of this element include compact size, simple structure, wide passband, and wide stopband. Thus, this parallel coupled line topology is suitable for compact UWB BPF design. The proposed design consists of 2-parallel coupled lines with a T-inverted shape. The designed filter has two identical parallel lines with an electrical length of about a quarter wavelength at the desired center frequency. The third line is centred between the two extreme lines with different lengths and widths, in which a rectangular shape is attached at its end to form a T-inverter shape (Because the shape of the middle-line resembles the inverted letter

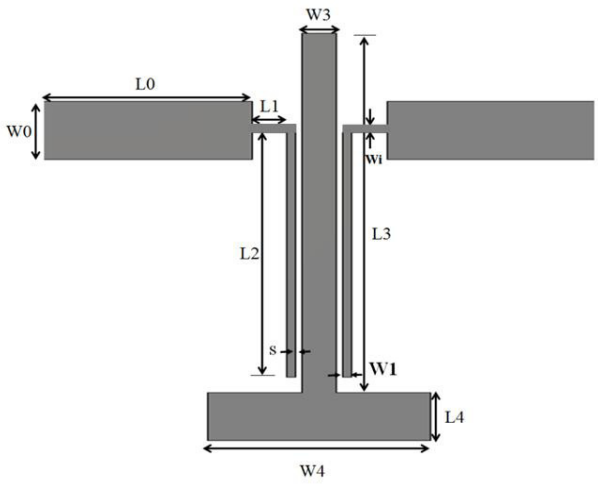

Figure 1. Geometry of the proposed bandpass filter.

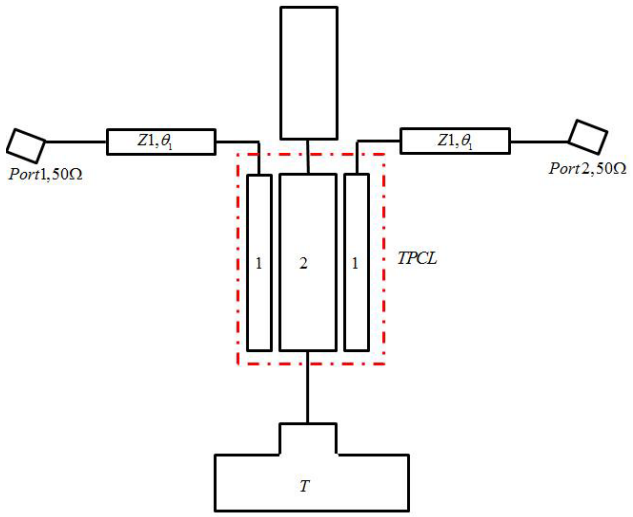

Figure 2. The equivalent transmission line model of the proposed filter.

"T", the coupled line is called an inverted T-shaped). The width of the middle line is $W3$, and $W1$ is the width of the two extreme other lines. The lengths of the middle line at the left- and right-hand sides are $L3$ and $L2$, respectively. The above elements are spaced by gap spacing S. An equivalent circuit of the bandpass filter demonstrated in this paper is shown in Fig. 2. The notations, TPCL in Fig. 2, represent three parallel coupled lines with small gap spacing, with Z_1 the characteristic impedance and θ_1 the electrical length of the line. Fig. 1 illustrates the geometry and configuration of the proposed filter, which is printed on an FR4 substrate with a dielectric constant $\epsilon r = 4.4$, substrates thickness $h = 1.58\,\text{mm}$, copper thickness $t = 35\,\mu\text{m}$, and tangent loss $\tan\delta = 0.025$. The characteristic impedance of the microstrip feed line was taken as $50\,\Omega$.

3. PARAMETRIC STUDIES

The parametric study is carried out to optimize the filter and provide more information about the effects of the essential design parameters. The filter performance is mainly affected by geometrical parameters, such as the length of the T-inverted shape, the length of the two extreme resonators, and the gap between resonators. In the first step design and in order to obtain the desired fractional bandwidth at the center frequency of 3.5 GHz, the designing method is based on software-oriented simulations focusing on realizing size reducing, low insertion loss, good matching over the whole frequency band. By installing the T-inverted shape with different lengths between the two extreme lines, three extra transmission zeros are excited after the desired passband, while the first three resonances are allocated into the passband. To clarify the proposed filters design, the design procedures of the wideband bandpass filter can be summarized as: (1) Based on the equivalent model, choose the desired center frequency f_0 of the bandpass filter, determine the four transmission zeros locations close to the passband; (2) Adjust

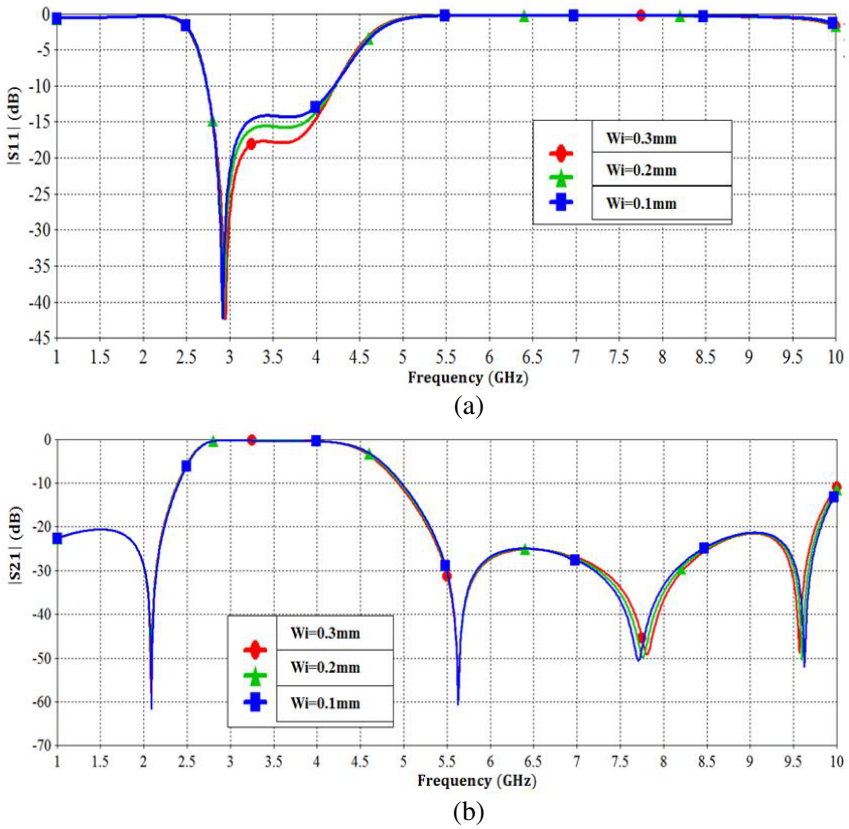

Figure 3. The effect of $W1$ (width of extreme line) on the proposed filter response. (a) Effect on return loss $|S11|$. (b) Effect on insertion loss $|S21|$.

the gap spacing between the parallel lines (s) to realize the desired bandwidth, choose the desired bandwidth for the filter (3-dB bandwidth greater than 50%, ($|S11| < -20\,\text{dB}$), out-of-band harmonic suppression ($|S21| < -20\,\text{dB}$). Furthermore, for optimizing the values of $L2$, $L3$ to realize better in-band and out-of-band transmission characteristics of the designed filter, full-wave electromagnetic simulation and dimension optimization are carried out in the commercial software of CST-MWS.

3.1. Effect of the Characteristic Impedance on the Filter Performance

To describe the effect of the characteristic impedance over the filter performances, we have maintained its parameters fixed and changed $W1$. Figs. 3(a), (b) show the variation response of return and insertion losses by varying $W1$ from 0.1 mm to 0.3 mm. From the graphs, we can see clearly that the return loss increases when $W1$ is increased; however, good matching input impedance around the center frequency is obtained when the $W1$ is fixed at 0.2 mm.

3.2. Effect of the $L2$ Length on the Performances

Furthermore, the effect of the extreme parallel lines length over the filter performances is evaluated. This time, we have proceeded to the change of length $L2$ by maintaining $W = 0.2\,\text{mm}$. Fig. 4 shows the variation of insertion loss. When $L2$ increases from 12.6 mm to 13.1 mm, the return losses become more matched and centred at the desired frequency of 3.5 GHz, and the bandwidth is also decreased slightly at the higher frequencies. The location of transmissions zeros as a function of $L2$ is shown in Fig. 4.

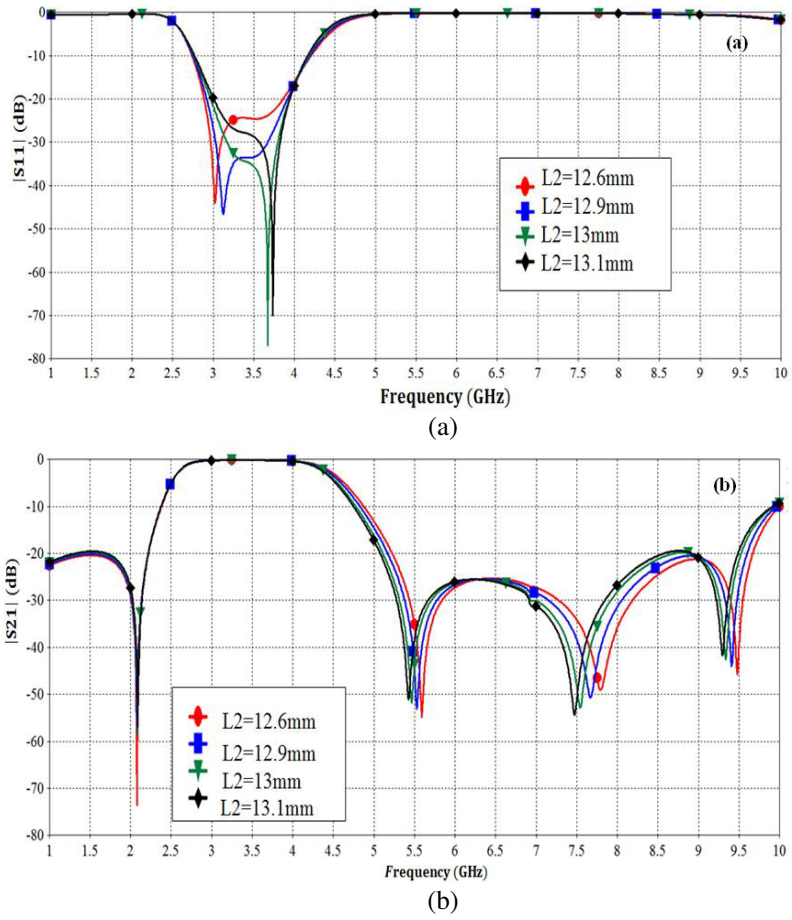

Figure 4. The effect of $L2$ (width of extreme line) on the proposed filter response. (a) Effect on return loss $|S11|$, (b) Effect on insertion loss $|S21|$.

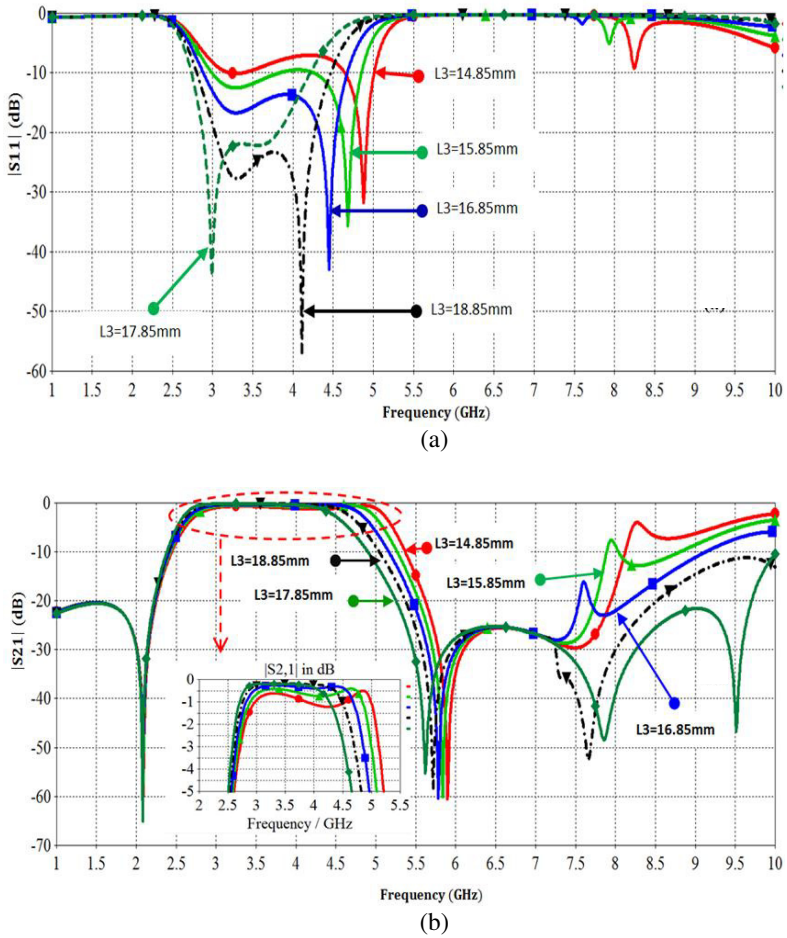

Figure 5. The effect of $L3$ on S-parameter of the proposed filter.

3.3. Effect of the $L3$ Length on the Performance

In order to widen the stopband of the filter significantly, $L3$ is increased. The harmonic suppression of the proposed bandwidth bandpass filter is extended to 9.7 GHz with a rejection level higher than 20 dB (see Fig. 5). We overcome this difficulty by connecting a multiple-mode parallel-coupled line structure with the rectangular resonator to build a wideband bandpass filter. This novel configuration of the filter is much smaller. Moreover, an extremely wide rejection band is achieved. As can be seen, increasing length $L3$ of the middle line shifts the second and third transmission zeros to lower frequencies and vice versa, and the fourth transmission zero appears. Basically, changing the length of this line should only affect the second, third and fourth transmission zeros. Therefore, the third and fourth transmission zeros appear and are also shifted to a lower frequency band. Moreover, the designed filter has excellent stopband performance. As a result, the upper rejection bandwidth is obtained from 5.25 GHz to 10.0 GHz; all are over 20 dB band rejections. It can also be seen that the out-of-band rejection level is below 20 dB at the lower band stopband (from DC to 2.2 GHz). Three transmission zeros are created to improve the selectivity and upper stopband performance. In addition, a good stopband rejection up to $3.f_0$ is obtained by increasing the length of the T-inverted shape structure where f_0 is the center frequency. The passband and stopband characteristics, together with compact dimensions of the proposed filter are evidence of its applicability in modern communication systems. It is also much easier to fabricate and more compact. The tail length of the T-inverted shape has been optimized using simulation with its width maintained at 0.82 mm, and the entire length of the shape has been optimized using parameter sweep simulation to obtain a wide stopband in the higher

frequencies. Due to the transmission zeros in the lower and upper stopbands, the filter exhibits good performance including sharp attenuations near the passband, and an extremely wide stopband, together with low insertion and return losses in the passband. All dimensions were adjusted by optimization processes to obtain the desired performances. A parametric study has been conducted to optimize the design of the filter. This study is crucial because it gives an approximation of design dimensions before the fabrication filter. Fig. 6 presents the current distribution for the proposed filter at two different frequencies. The first frequency is located in the passband at 3.5 GHz while the second is located in the stopband at 5.6 GHz. This study is very important because it gives us an idea about the critic geometrical parameters that can influence the behavior of the whole circuit. Along the transmitting region (3.5 GHz), the current distribution is the dominant (Fig. 6(a)). Contrariwise, at 5.6 GHz, the maximal RF current concentrates near the first line, and thus, no energy flows can transmit from the input to output of the filter (Fig. 6(b)).

Table 1. Variation of the attenuation pole and insertion loss with a dimension of T-inverted shape structure.

Length of $L3$ (mm)	Width $W3$ (mm)	Attenuation Pole (GHz)	Insertion loss (dB)
14.85	0.82	5.89	−0.62
15.85	0.82	5.84	−0.46
16.85	0.82	5.77	−0.27
17.85	0.82	5.71 and 7.66	−0.16
18.85	0.82	5.61, 7.85 and 9.5	−0.19

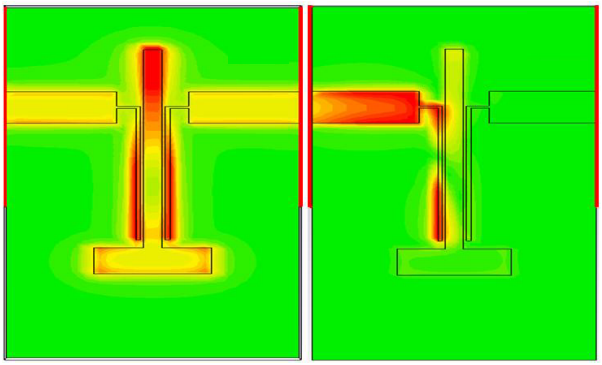

Figure 6. Presents the current distribution. (a) pass-band at 3.5 GHz and (b) reject band at 5.6 GHz.

4. FABRICATED FILTER AND MEASUREMENT

Following the guidelines described in the previous section and in order to verify the simulated results obtained by CST-MWS solver, the filter is fabricated on a low-cost FR4 substrate by using LPKF machine and measured using MS2028C Anritsu VNA in microwave laboratory. A photograph of the fabricated filter is shown in Fig. 7.

To create an input and an output ports, two SMA connectors were soldered to the feed lines. The outer dimension of the prototype model was 13.24 mm × 23.30 mm. The related dimensions of the final BPF as shown in Fig. 1 are determined as follows (all in mm), including $W0 = 2.97$, $L0 = 5$, $L1 = 0.85$, $L2 = 12.5$, $L3 = 18.35$, $L4 = 2.45$, $W1 = 0.2$, $W3 = 0.82$, $W4 = 5.34$, and $S = 0.2$. The simulated lower and upper 3-dB cut-off frequencies are calculated approximately at 2.53 GHz and 4.56 GHz, respectively. The total 3-dB transmission bandwidth of the filter is 2.03 GHz. The simulated

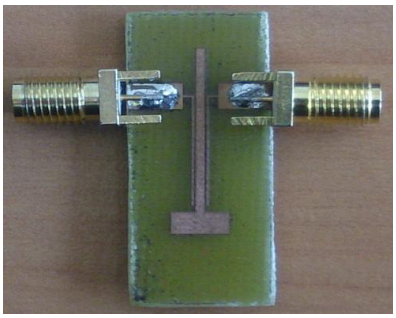

Figure 7. Photograph of the fabricated bandpass filter.

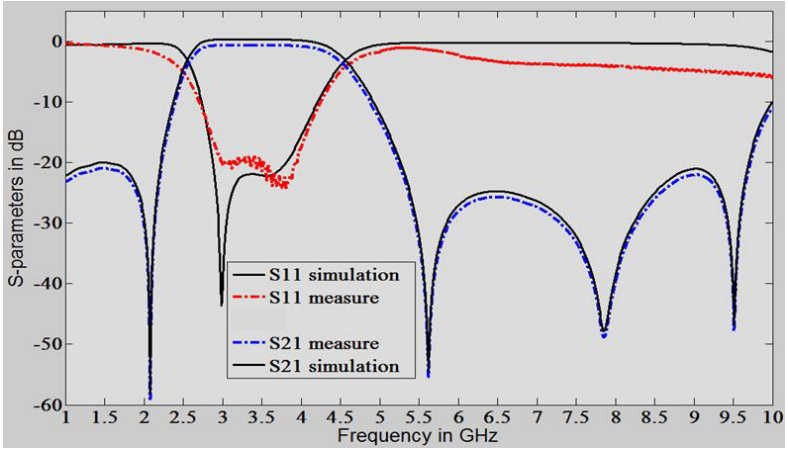

Figure 8. Simulated and measured results of fabricated wideband bandpass filter.

and measured results for the designed filter obtained using CST-Studio software and an MS2028C Anritsu VNA (Master Vector Network Analyzer) are presented. The simulated and measured results at the frequency range from 1 to 10 GHz are shown in Fig. 8. The agreement between the measurement and design simulation is observed. The measured center frequency of the filter is about 3.5 GHz, and the 3-dB fractional bandwidth is about 62.75%. Within the passband, the return loss is better than 20 dB at most frequencies, while the insertion losses of the filter are less than 1-dB. The transmission zeroes obtained from circuit implementation were 2.04, 5.63, 7.9 and 9.5 GHz for the passband. Furthermore, an upper stopband over -22 dB was achieved from 5.25 to 9.7 GHz, indicating excellent wideband suppression. The result, presented in Fig. 8, shows that the filter has a wide flat passband together with deep transmission zeros just below and above the passband. Although a slight difference at the higher frequencies can be observed, this mismatch can be explained by an error in the manufacturing process or/and a variation in the material properties. In fact, the fabrication tolerances, as well as the SMA connectors and the calibration errors, may have led to the discrepancies between the simulated and measured results in the upper stopband. The group delay varies from 0.30 to 0.56 ns. In other words, the maximum variation in group delay achieves 0.56 ns, indicating a good linearity of the developed filter.

The group delay of this wide-band bandpass filter can be calculated by:

$$\tau = \frac{-\partial \angle S_{21}}{\partial \omega} \tag{1}$$

where $\angle S_{21}$ is the insertion loss phase and ω the frequency in radians per second. Fig. 9 shows the group delay of the filter. Within the passband, the group delay is below 1 ns. Table 2 presents simulations and measurements of the proposed filter.

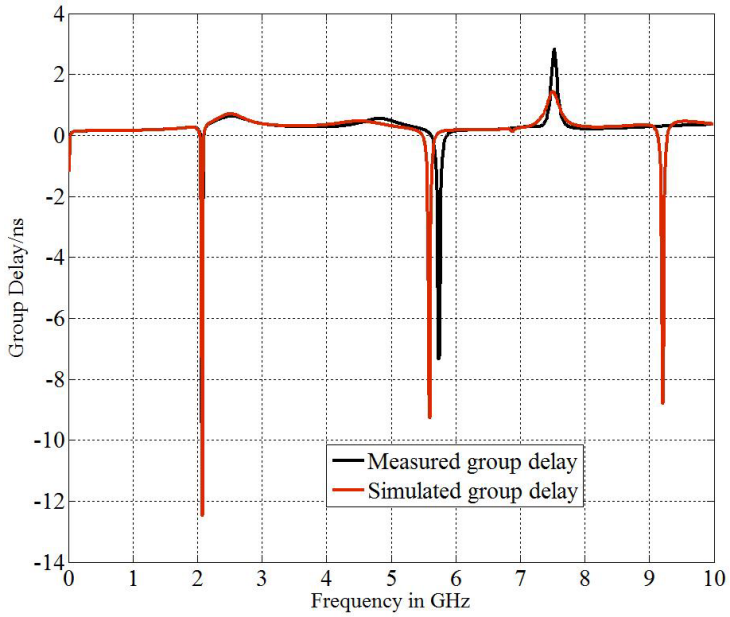

Figure 9. Group delay of the designed filter.

Table 2. Simulations and measurements results of the proposed filter.

	Simulations	Measurements
Fc in GHz	3.5	3.52
FBW%	70	62.75
Transmission zeros	2.08, 5.61, 7.85, 9.5 GHz	2.08, 5.61, 7.85, 9.51 GHz
Return Loss	22.14 dB	21.5 dB
Insertion Loss	−0.3 dB	−0.69 dB
Group Delay	0.32 ns	0.25 ns
Stopband @ 20 dB	5.26–9.7 GHz	5.25–9.72 GHz
RSB	59.35%	59.7%

Table 3. Comparison of this work with others.

Ref.	fc in GHz	FWB%	R.L dB	I.L dB	G.Delay ns	U-STB	Size (mm^2), λ_g
This work	3.5	70	20	0.7	0.42	5.2–9.7	$13.24 \times 23.30\,mm^2$
[4]	2.4	25	25	< 2	—	3.1–6	$10 \times 5\,mm^2$
[9]	3	43.3	17	0.6	—	3.75–7.5	$(0.1 \times 0.13)\lambda_g$
[11]	2.99	61.7	15	—	0.7	4.56–8.02	$51 \times 40\,mm^2$, $(0.68 * 0.53)\lambda_g$
[12]	2.08	26.8	17.2	0.65	—	2.5–3.5	$50 \times 59\,mm^2$
[13]	5.02	36.1	18	0.4	—	6.4–7	$17.7 \times 18\,mm^2$, $(0.39 * 0.41)\lambda_g$
[18]	4.25	54	15	0.5	0.2	6.3–10	—
[19]	5	75	11.5	0.4	0.29	7.2–11.7	$22.6 \times 8.2\,mm^2$
[20]	2.9	69.5	10	1.55	1.77	> 15	$(0.472 \times 0.324)\lambda_g$
[21]	4.3	68	13	1.31	0.62–0.98	—	—

where λ_g is the guided wavelength at f_0 which is the center frequency of the proposed BPF.

The relative stopband width (RSB) is:

$$RSB = \frac{Stopband}{Stop\ Center\ Frequency} \tag{2}$$

Table 3 is provided for comparison of this work with other works which are all based on wide-band bandpass filter category.

5. CONCLUSION

The paper presents a compact structure of wideband bandpass filter with wide stopband using only two parallel coupled lines and a T-inverted shape. The circuit performance in the rejection band was improved by suppressing the harmonic peaks with T-shaped transmission lines by changing its length. A wideband bandpass filter with harmonic suppression was manufactured easily. This proposed WBPF at 3.5 GHz was fabricated and measured, showing good characteristics including wide bandwidth of 70%, four transmission zeros in the passband edge and wide stopband rejection below 2.2 GHz and from 5.2 to 9.7 GHz. The measurement results are in agreement with simulation, which validates this filter for WiMAX applications. The total dimensions of this filter are $13.24 \times 23.30\ mm^2$ which will allow this circuit to be used in various wideband wireless applications.

REFERENCES

1. Hong, J. S., *Microstrip Filters for RF/Microwave Applications*, Wiley, New York, 2011.
2. Lei, Z., S. Sheng, and R. Li, *Microstrip Filters for Rf/Microwave Applications*, Wiley, New Jersey, 2012.
3. Zhang, R. and L. Zhu, "Synthesis design of a wideband bandpass filter with inductively coupled short-circuited multi-mode resonator," *IEEE Microwave and Wireless Components Letters*, Vol. 22, No. 10, 509–511, Oct. 2012.
4. Wu, X.-H., X.-B. Wei., H.-G. Lv., and Y. Shi, "Compact bandpass filter with multiple transmission zeros using modified stepped-impedance resonators," *Journal of Electromagnetic Waves and Applications*, Vol. 29, No. 13, 1741–1748, Oct. 2015.
5. Wu, C.-H., Y.-S. Lin, C.-H. Wang, and H. C. Chun, "Compact microstrip coupled-line bandpass filter with two cross-couplings for creating multiple transmission zeros," *European Microwave Conference* , Oct. 4–6, 2005.
6. Wang, H., Q. X. Chu, and J. Q. Gong, "A compact wideband microstrip filter using folded multiple-mode resonator," *IEEE Microwave and Wireless Components Letters*, Vol. 19, No. 5, 287–289, 2009.
7. Ma, X.-B. and T. Jiang, "Wideband bandpass filter with controllable bandwidth and high selectivity using two different types of resonators," *Microw. Opt. Technol. Lett.*, Vol. 57, No. 6, 1319–1323, 2015.
8. Yu, C. C., C.-H. Kao, M.-H. Weng, and R.-Y. Yang, "Design of the compact wideband bandpass filter with low loss, high selectivity and wide stopband," *IEEE Microwave and Wireless Components Letters*, Vol. 18, No. 12, 770–772, 2008.
9. Huang, Y. J.-M., B. Zhang, and S. S. Li, "Novel compact quad-mode wideband bandpass filter with wide stopband using T-shaped resonator," *Journal of Electromagnetic Waves and Applications*, Vol. 28, No. 3, 326–333, 2014.
10. Feng, W., X. Gao, and W. Che, "Bandpass filters with improved selectivity based on dual-mode ring resonators," *Progress In Electromagnetics Research Letters*, Vol. 56, 1–7, 2015.
11. Feng, W. J., W. Q. Che, Y. M. Chang, S. Y. Shi, and Q. Xue, "High selectivity fifth-order wideband bandpass filters with multiple transmission zeros based on transversal signal-interaction concepts," *IEEE Transactions on Microwave Theory and Techniques*, Vol. 61, No. 1, 89–97, 2013.
12. Chen, H. and H. Zhao, "A novel microstrip bandpass filter with an elliptic-function response using improved dual-stub resonator," *Journal of Electromagnetic Waves and Applications*, Vol. 29, No. 16, 2224–2231, 2015.

13. Chen, H., P. Tang, K Chen, H. Zhao, and H. Zhong., "Wideband dual-mode bandpass filter using a modified right-triangular patch resonator overlapped with input/output DMS," *Journal of Electromagnetic Waves and Applications*, Vol. 27, No. 11, 1365–1371, 2013.
14. Feng, W.-J., X. Gao, and W.-Q. Che, "Bandpass filters with multiple transmission zeros using open/shorted stubs," *IET Microwave Antennas Propag.*, Vol. 9, No. 8, 769–774, 2015.
15. Park, J. S., J. S. Yun, and D. Ahn, "A design of the novel coupled-line bandpass filter using defected ground structure with wide stopband performance," *IEEE Trans. Microw. Theory Tech*, Vol. 50, No. 9, 2037–2043, 2002.
16. Boutejdar, A., A. Elsherbini, and A. S. Omar, "Method for widening the reject-band in low-pass/band-pass filters by employing coupled C-shaped defected ground structure," *IET Microwaves. Antennas Propag.*, Vol. 2, No. 8, 759–765, 2008.
17. Boutejdar, A., A. Batmanov, A. Omar, and E. Burte, "A miniature 3.1 GHz microstrip bandpass filter with suppression of spurious harmonics using multilayer technique and defected ground structure open-loop ring," *Ultra-Wideband, Short Pulse Electromagnetics*, Vol. 9, 171–178, 2010.
18. Song, K. and Q. Xue, "Novel broadband bandpass filters using Y-shaped dual-mode microstrip resonators," *IEEE Microw. Wirel. Components Lett.*, Vol. 19, No. 9, 548–550, 2009.
19. Luo, X., H. Qian, J.-G. Ma, and E.-P. Li, "Wideband bandpass filter with excellent selectivity using new CSRR-based resonator," *Electron. Lett.*, Vol. 46, No. 20, 1390–1391, 2010.
20. Mandal, M. K. and S. Sanyal, "Design of wide-band, sharp-rejection bandpass filters with parallel-coupled lines," *IEEE Microw. Wirel. Components Lett.*, Vol. 16, No. 11, 597–599, 2006.
21. Chaimool, S. and P. Akkaraekthalin, "Miniaturized wideband bandpass filter with wide stopband using metamaterial-based resonator and defected ground structure," *Radioengineering.*, Vol. 21, No. 2, 611–616, 2012.